# Dual single-scission event analysis of constitutive transferrin receptor (TfR) endocytosis and ligand-triggered β2-adrenergic receptor (β2AR) or Mu-opioid receptor (MOR) endocytosis

Marko Lampe[a,b], Fabienne Pierre[c], Suleiman Al-Sabah[d], Cornelius Krasel[e], and Christien J. Merrifield[c]

[a]European Molecular Biology Laboratory, 69117 Heidelberg, Germany; [b]Translational Lung Research Center, Department of Translational Pulmonology, University of Heidelberg, 69120 Heidelberg, Germany; [c]Centre National de la Recherche Scientifique UPR3082, Laboratoire d'Enzymologie et de Biochimie Structurales, 91198 Gif-sur-Yvette Cedex, France; [d]Department of Pharmacology and Toxicology, Faculty of Medicine, Kuwait University, 13110 Safat, Kuwait; [e]Fachbereich Pharmazie, Institut für Pharmakologie und Klinische Pharmazie, Philipps-Universität Marburg, 35033 Marburg, Germany

**ABSTRACT** **The dynamic relationship between constitutive and ligand-triggered clathrin-mediated endocytosis is only poorly characterized, and it remains controversial whether clathrin-coated pits specialize to internalize particular receptor cargo. Here we analyzed the ligand-triggered endocytosis of the model G-protein–coupled receptors (GPCRs) β2-adrenergic receptor (β2AR) and Mu-opioid receptor (MOR) at the level of individual endocytic events using a total internal reflection fluorescence microscopy (TIRFM)–based assay. Similar to the constitutive endocytosis of transferrin receptor (TfR), ligand- triggered endocytosis of β2AR occurs via quantized scission events hosted by clathrin spots and plaques of variable size and persistence. To address whether clathrin-coated structures (CCSs) specialize to internalize particular GPCRs, we adapted the TIRFM imaging assay to simultaneously quantify the internalization of TfR and the ligand- triggered endocytosis of the β2AR or MOR. Agonist-triggered β2AR or MOR endocytosis extended the maturation time of CCSs, as shown previously, but did not affect the rate of constitutive TfR endocytosis or loading of TfR into individual endocytic vesicles. Both the β2AR and the MOR receptors entered cells in the same vesicles as TfR, and the overall evidence for CCS specialization was weak. These data support a simple model in which different cargoes internalize through common CCSs.**

**Monitoring Editor**
David G. Drubin
University of California, Berkeley

Received: Jun 17, 2014
Revised: Jul 18, 2014
Accepted: Jul 18, 2014

## INTRODUCTION

Clathrin-mediated endocytosis is the main pathway for receptor internalization in eukaryotic cells. In this well-conserved pathway, receptors concentrate at clathrin-coated pits through association with adaptors and internalize as coated pits invaginate and bud into the cell. Total internal reflection fluorescence microscopy (TIRFM) has become an important tool to analyze the spatial and temporal organization of clathrin-mediated endocytosis in living cells (Rappoport, 2008). However, there remains some controversy over what constitutes a "canonical" clathrin-coated pit in live-cell imaging studies. Some studies suggest that receptor-mediated endocytosis is restricted to discrete, punctate clathrin-coated pits, whereas larger and more stable clathrin plaques are endocytically inactive (Batchelder and Yarar, 2010) or constitute a unique pathway of endocytosis (Saffarian *et al.*, 2009). However, when individual constitutive endocytic events of transferrin receptor (TfR), tagged with pH-sensitive super-ecliptic pHluorin (sePhl; Sankaranarayanan and Ryan, 2000), were imaged directly using a TIRFM-based "pulsed pH"

This article was published online ahead of print in MBoC in Press (http://www.molbiolcell.org/cgi/doi/10.1091/mbc.E14-06-1112) on July 30, 2014.

Address correspondence to: Christien J. Merrifield (christien.merrifield@lebs.cnrs-gif.fr).

Abbreviations used: β2AR, β2-adrenergic receptor(s); CCS, clathrin-coated structure(s); GPCR, G-protein–coupled receptor(s); MOR, mu-opioid receptor(s); TfR, transferrin receptor(s); TIRFM, total internal reflection fluorescence microscopy.

assay, it was found that both punctate coated pits and larger plaques could host multiple discrete, quantized scission events (Merrifield *et al.*, 2005; Taylor *et al.*, 2011). The pulsed pH assay identified individual scission events using the occlusion of fluorescently tagged, pH-sensitive receptor cargo from rhythmically imposed external pH changes (Merrifield *et al.*, 2005; Taylor *et al.*, 2011). Here we used the pulsed pH assay to determine the physical characteristics of clathrin-coated structures (CCSs) that endocytosed the two model G-protein–coupled receptors (GPCRs) β2-adrenergic receptor (β2AR) and Mu-opioid receptor (MOR).

A second point of controversy is whether clathrin-coated pits can specialize to internalize specific cargo to the exclusion of other types of receptor. It has been suggested that CCPs can specialize to internalize different types of GPCR (Mundell *et al.*, 2006) or to internalize particular GPCRs while excluding TfR, which implies that receptor sorting can start at the plasma membrane (Cao *et al.*, 1998; Tosoni *et al.*, 2005; Puthenveedu and von Zastrow, 2006). In an alternative model, all CCPs are capable of internalizing a mixture of receptor cargo via a variety of receptor-specific adaptor proteins (Keyel *et al.*, 2006), and receptor sorting begins only after internalization (Burd and Cullen, 2014).

To probe the dynamic relationship between constitutive and ligand-triggered receptor-mediated endocytosis and to quantitatively analyze the cointernalization of different types of receptor at individual scission events, we extended the pulsed pH assay to simultaneously image two different receptors, with the TfR labeled green (with sePhl) and either β2AR or MOR labeled red with the moderately pH-sensitive fluorescent protein mApple (Shaner *et al.*, 2008).

## RESULTS

### Single-event detection of β2-adrenergic receptor endocytosis

To measure the dynamics of constitutive clathrin-mediated endocytosis in HEK293 cells, we used an optical assay to detect single-scission events of TfR (Merrifield *et al.*, 2005; Taylor *et al.*, 2011). Briefly, TfR was tagged at the extracellular domain with super-ecliptic pHluorin, a pH-sensitive variant of green fluorescent protein (Miesenbock *et al.*, 1998; Sankaranarayanan and Ryan, 2000) to produce TfR-phl (Merrifield *et al.*, 2005). A large-diameter perfusion tip was brought close to the target cell, and perfusate was cycled between buffer of pH 7.4 and 5.5 in synchrony with image acquisition at 0.5 Hz using dual-color TIRFM (Merrifield *et al.*, 2005; Taylor *et al.*, 2011; Supplemental Figure S1A). Scission events manifested as the abrupt appearance of pH-resistant TfR-phl punctae in images acquired at pH 5.5, colocalized with CCSs labeled with mCherry-tagged clathrin light chain (Clc-mCherry; Supplemental Figure S1A).

To detect single ligand-triggered endocytic events, we tagged the model GPCR β2AR at the extracellular N-terminus with super-ecliptic pHluorin to make phl-β2AR. The hemagglutinin leader sequence was inserted N-terminal to pHluorin to ensure the correct membrane insertion of the receptor (see *Materials and Methods*). As shown in an earlier study, attachment of pHluorin in front of the extracellular domain had negligible effects on the pharmacokinetics of ligand-triggered β2AR endocytosis (Puthenveedu *et al.*, 2010). To detect single-scission events, we used a perfusion system (Taylor *et al.*, 2012) to integrate rhythmic changes of extracellular pH with controlled perfusion of the β2AR agonist isoproterenol, which rapidly triggers β2AR signaling and endocytosis (Staehelin and Simons, 1982; Supplemental Figure S1, B–D). Hence potential scission events could be detected while isoproterenol was washed on, and then off, the target cell.

In an example HEK293 cell coexpressing green phl-β2AR and Clc-mCherry, phl-β2AR fluorescence was homogeneous across the plasma membrane and did not colocalize with punctate CCSs (Figure 1Ai). The cell was imaged with pH cycling for 250 s, and in an example image acquired at pH 5.5, no pH-resistant phl-β2AR was detected close to the plasma membrane (Figure 1Ai). At 250 s, the perfusion stream was switched to buffers containing 20 μM isoproterenol, which triggered rapid recruitment of phl-β2AR into CCSs (Figure 1Ai). In an example image acquired at pH 5.5, a population of brightly fluorescent punctae was revealed colocalized with Clc-mCherry labeled CCSs and with patches of phl-β2AR at pH 7.4 (Figure 1Aii, yellow circles). Not all clathrin patches colocalized with a correlated spot of phl-β2AR at pH 7.4 (Figure 1Aii, white arrowhead). These rare CCSs could represent coated pits that entirely lacked phl-β2AR (Cao *et al.*, 1998), or they could be CCSs that pinched of at pH 5.5 or otherwise naturally acidified after scission; in either of the latter cases, the phl-β2AR cargo would be quenched and therefore invisible. The pH-resistant spots of phl-β2AR fluorescence in images acquired at pH 5.5 represented newly formed endocytic vesicles containing phl-β2AR that pinched off of the plasma membrane as the cell was perfused with a pulse of buffer at pH 7.4 in the preceding image (Figure 1Aii, yellow circles).

Phl-β2AR(+) scission events manifested as the abrupt appearance of pH 5.5–resistant phl-β2AR spots colocalized with a cluster of phl-β2AR at pH 7.4 (Figure 1B). To quantify scission events, we used a semiautomated analysis similar to one described previously (Taylor *et al.*, 2011). Acid-resistant phl-β2AR spots were tracked, their fluorescence quantified, and bona fide scission events classified primarily on the ratio of signal to noise (S/N) of the step increase in fluorescence (Figure 1B).

The rapid clustering of phl-β2AR at CCSs was coordinated with a burst of detected scission events in images acquired at pH 5.5 (Figure 1C, gray histogram). Analysis of a cumulative frequency plot ($n$ = 1986 events, $N$ = 3 cells) revealed a remarkably steady flux of scission events for the duration of isoproterenol exposure (Figure 1C, blue line). At $t$ = 850 s, the perfusion stream was switched back to buffer lacking isoproterenol, after which the rate of scission events tailed off over ~200 s (Figure 1C).

### β2AR(+) scission events occurred at clathrin spots and plaques

The dynamic characteristics of endocytically active CCSs and the relationship between clathrin-coated bud maturation and CCS lifetime remains only poorly appreciated (for discussion see Mooren *et al.*, 2012). In general, endocytically active CCSs at the adherent surface of cells were considered to be discrete, punctate CCSs that nucleated, grew in fluorescence, maintained a stable plateau of fluorescence for some variable time (mean, ~50 s), and abruptly disappeared upon internalization (Merrifield *et al.*, 2002; Ehrlich *et al.*, 2004; Loerke *et al.*, 2009). Larger, persistent clathrin plaques were considered either to be endocytically inactive (Batchelder and Yarar, 2010) or to be involved in a different, "noncanonical" clathrin-mediated endocytic pathway (Saffarian *et al.*, 2009). However, there is also evidence that the distinction of size classes of CCS is almost superfluous with regard to clathrin-coated bud formation because in NIH3T3 cells, quantized TfR(+) scission events were hosted by both discrete, punctate CCSs and larger and more persistent clathrin patches, and either type of structure could potentially host multiple scission events (Merrifield *et al.*, 2005; Taylor *et al.*, 2011).

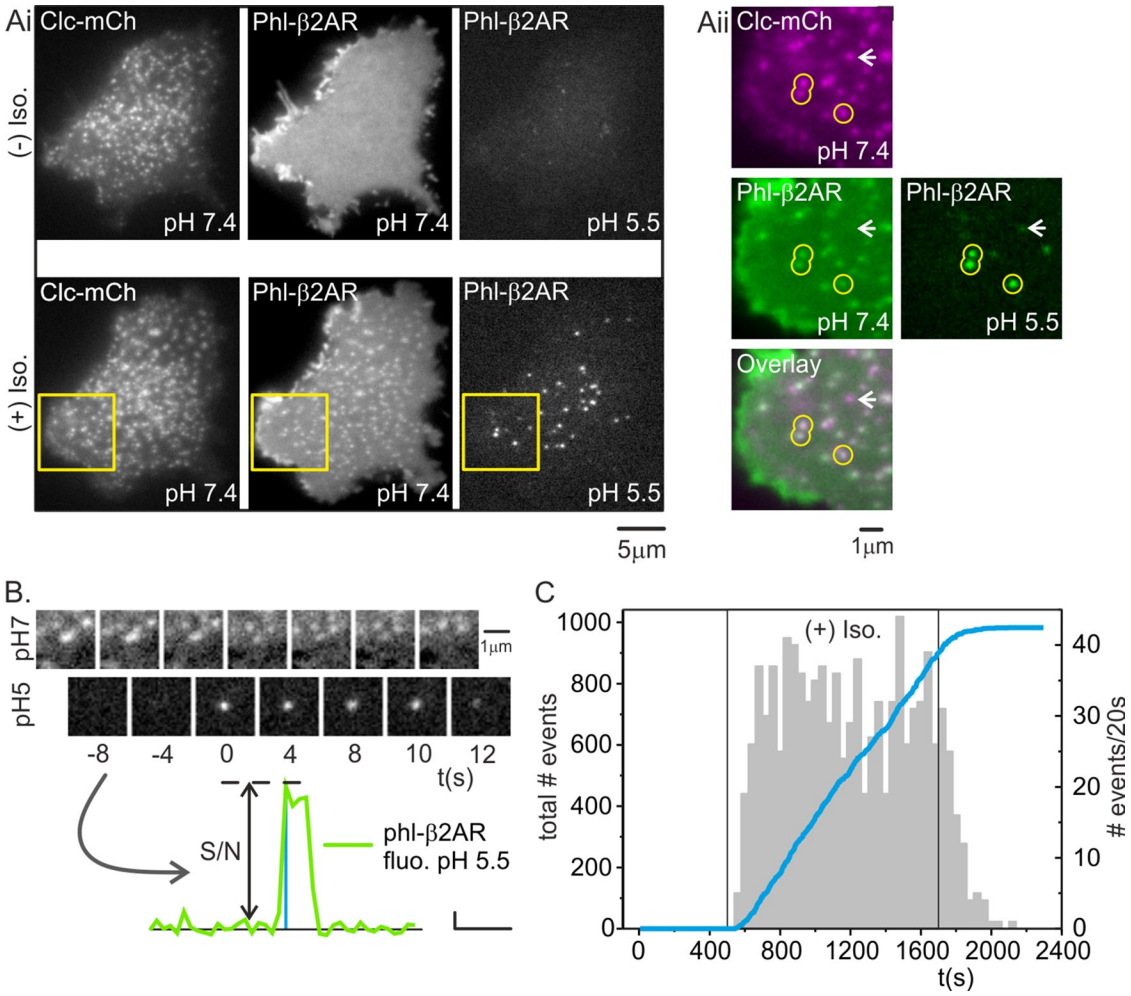


FIGURE 1: Single-event analysis of β2AR internalization. (Ai) Example HEK293 cell expressing Clc-mCh (left) and phl-β2AR at pH7.4 (middle) and 2 s later at pH 5.5 (right); first image taken ~428 s before addition of isoproterenol. At pH 5.5, cell-surface phl-β2AR quenched and no pH-resistant, phl-β2AR(+)endosomes were visible close to the plasma membrane. (Aii) Same cell 240 s after addition of isoproterenol. Phl-β2AR became concentrated at coated pits at pH 7.4 (middle). When cell-surface phl-β2AR was quenched 2 s later at pH 5.5, acid-resistant endosomes containing phl-β2AR were clearly visible close to the plasma membrane. (Aiii) Expanded region indicated in Aii, showing Clc-mCh (magenta, top left), phl-β2AR at p H7.4 (green, middle left), and overlay (lower left). Three acid-resistant, phl-β2AR(+) endosomes were visible in the field (green, middle right) colocalized with CCS (yellow circles). (B) Time-resolved images of a single-scission event engulfing phl-β2AR. The fluorescence was quantified and bona fide scission events defined primarily on the basis of S/N (lower graph, scale: vertical 2.5 a.u., horizontal 33 s; see *Materials and Methods* for details). (C) Time course of detected scission events before, during, and after addition of isoproterenol. Summarized data from four cells showing the incidence of scission events over a 20-s time window (gray histogram) and the cumulative number of scission events (blue line).

To define the dynamic characteristics of CCSs that hosted β2AR(+) scission events, we transfected HEK293 cells with phl-β2AR and Mu2-mCherry to label CCSs and detected and analyzed scission events as described. Similar to NIH3T3 fibroblasts, both spot-like CCSs and larger and longer-lived clathrin plaques could exist at the adherent surface of HEK293 cells (Figure 2A). Persistent clathrin plaques occurred in a significant proportion (~10%) of cells growing on fibronectin-coated coverslips and were most likely triggered by tight adhesion to the substrate (Batchelder and Yarar, 2010). On challenge with isoproterenol, phl-β2AR rapidly clustered at preexisting spot-like CCSs (Puthenveedu and von Zastrow, 2006) and large clathrin plaques (Figure 2, A and Bi). As shown earlier, not all punctate CCSs showed clear colocalization with phl-β2AR at pH 7.4 (Figure 1Aii), and fine, finger-like projections at the lower surface of some HEK293 cells obscured things further (Figure 2Ai). These background features were quenched at pH 5.5 and so did not interfere with the detection of CCSs or scission events. Strikingly, when β2AR(+) scission events were mapped to their host CCS, both clathrin punctae and clathrin plaques could host spot-like scission events (Figure 2, Bi and Bii). To quantify the distribution of scission events among spot-like CCSs and clathrin plaques for five cells, we segmented images (see *Materials and Methods*) and quantified the pixel area of the phl-β2AR(+)-marking scission and the corresponding "host" CCS, labeled with Mu2-mCherry, and plotted the result as a density scatterplot (Figure 2C). All scission events were the size of diffraction-limited spots, but a significant proportion (~10%) of clathrin objects hosting scission events were significantly larger blobs and so classified as "plaques." Therefore (and as shown previously for TfR-phl; Taylor *et al.*, 2011), both clathrin spots and plaques could host discrete, quantized scission events of phl-β2AR, and the

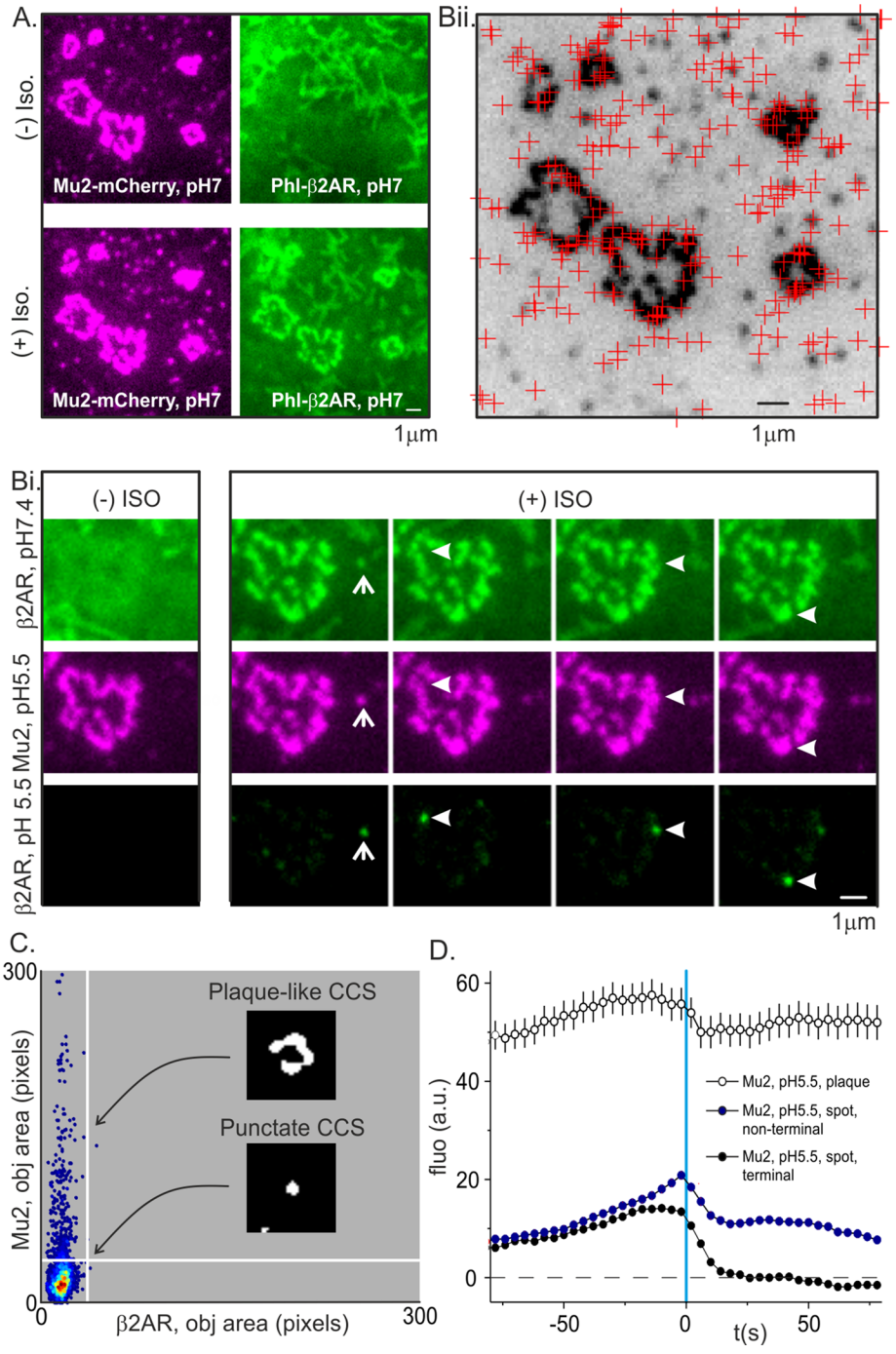


FIGURE 2: Discrete, quantized scission events internalized β2AR at clathrin spots and plaques. (A) An example HEK293 cell expressing the CCS marker Mu2-mCherry (magenta) and phl-β2AR (green) before (top) and after (bottom) challenge with isoproterenol. In this particular cell, CCSs appeared as discrete punctae and larger rosette-like plaques. (Bi) After challenge with isoproterenol, phl-β2AR was concentrated at both types of CCS, and discrete scission events were detected at either type of structure. (Bii) A map of detected scission events (red crosses) overlaid on an inverted image of Mu2-mCherry (black). Scission events were detected at both punctate CCSs and larger clathrin plaques. (C) Density scatterplot of Mu2-mCherry object area (ordinate) vs. newly scissioned phl-β2AR object area (abscissa). The fluorescence objects marking scission events are always spots but may colocalize to punctate or plaque-like CCSs. (D) Aligned and average fluorescence traces for Mu2-mCherry fluorescence at terminal punctate (black circles), nonterminal punctate (red circles), or plaque-like CCSs (open circles). All types of CCS show a drop in fluorescence after scission corresponding to CCV uncoating but differ in the persistence of fluorescence signal after scission.

relative sizes of clathrin spots and plaques are poor predictors of the endocytic potential of any given CCS. In previous studies, it was likely that the endocytic activity at the edges of clathrin plaques was masked by the bright fluorescence of the plaque itself and so remained undetected. This was verified when Mu2-mCherry fluorescence traces were classified according to whether they occurred at spots or plaques: the average fluorescence traces in each case showed a discrete dip after scission, presumably as the clathrin bud separated from the host structure and was uncoated (Figure 2D).

### Lifetimes analysis of spot-like CCS hosting β2AR(+) scission events

We next focused on a more detailed analysis of spot-like CCS lifetimes, since the dynamics of these structures are most readily analyzed, and the lifetime of spot-like coated pits was used previously as a readout of clathrin-coated pit maturation (Ehrlich *et al.*, 2004; Puthenveedu and von Zastrow, 2006; Loerke *et al.*, 2009; Henry *et al.*, 2012). To determine the maturation time of productive clathrin-coated buds, we tracked Mu2-mCherry labeled CCSs and mapped them to bona fide scission events (Merrifield *et al.*, 2005). As shown previously for TfR in fibroblasts (Merrifield *et al.*, 2005; Taylor *et al.*, 2011, 2012), spot-like CCSs most commonly hosted only one scission event but could potentially host multiple scission events (Figure 3, A and B). Strikingly, many scission events coincided with partial dimming but not complete disappearance of the host CCS, and repeated trains of partial dimming resulted in characteristic sawtooth-type profiles of Mu2-mCherry fluorescence (Figure 3A, right pair of traces). As described previously for NIH fibroblasts (Merrifield *et al.*, 2005; Taylor *et al.*, 2011), "nonterminal" events, for which the host CCS did not completely disappear after scission, comprised a significant proportion of the total number of scission events (~50%). By definition, terminal events coincided with the final disappearance of the host spot-like CCS (Figure 3A).

Clearly, the overall lifetime of a spot-like CCS is not an entirely accurate readout for the time course of clathrin-coated bud maturation. To estimate the time taken to form a productive clathrin bud, we measured the time between the first appearance (i.e., nucleation) of spot-like CCSs and their correlated first detected β2AR(+) scission event (Figure 3C). The median time was ~119.6s, which is ~53% longer than clathrin bud maturation in cells expressing only TfR-phl

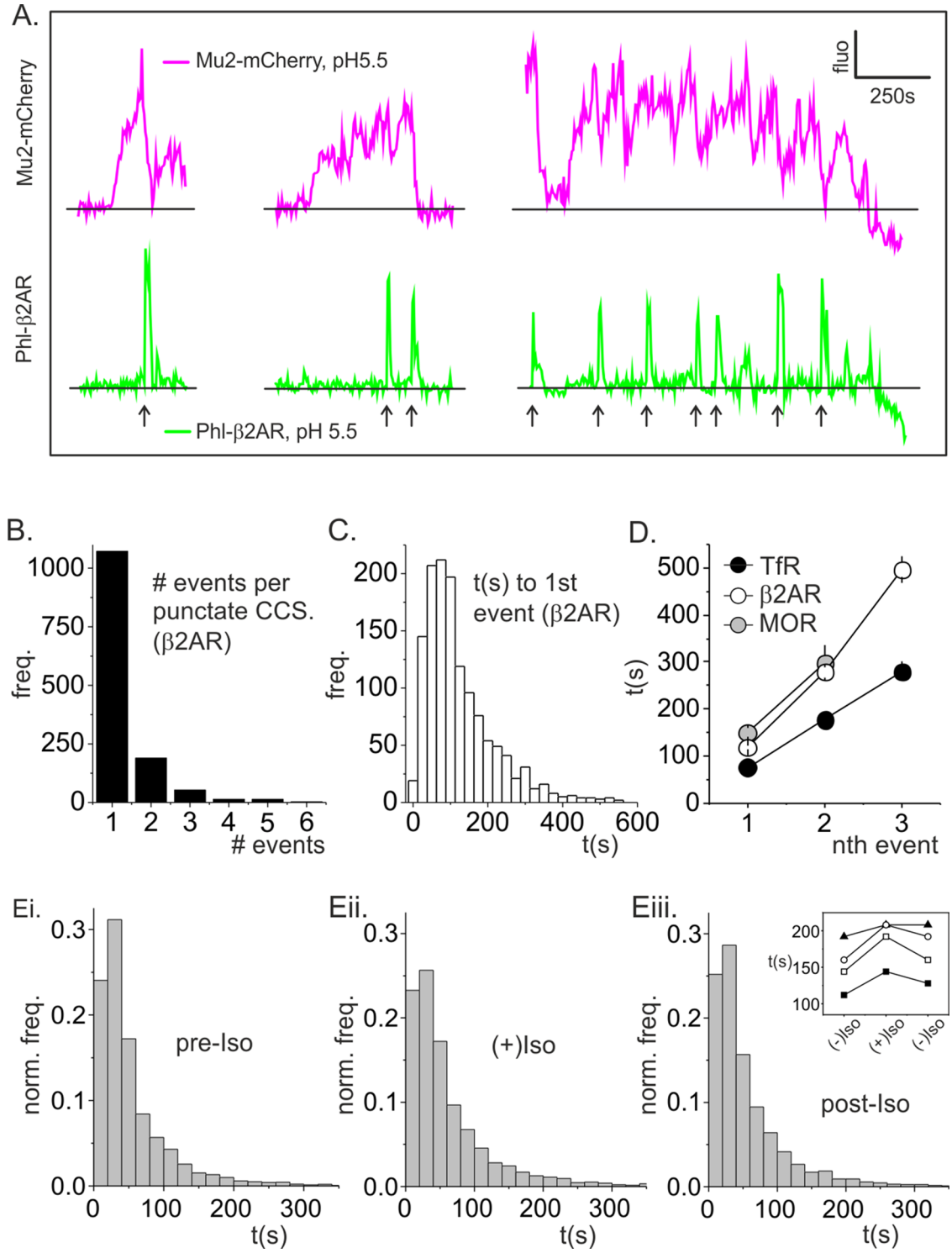


FIGURE 3: Lifetimes analysis of clathrin spots. (A) Example fluorescence traces for Mu2-mCherry (magenta) and phl-β2AR (green) for CCSs that hosted one, two, and seven scission events, respectively (arrows). (B) Histogram of the number of scission events detected per punctate CCS. A significant proportion (~20%) of punctate CCSs hosted more than one scission event. (C) Histogram of the time between CCS nucleation and the first detected scission event for β2AR (median lifetime, 119.6 s). (D) The time between CCS nucleation and the first, second, or third detected scission event for TfR(+) scission events (black circles), β2AR(+) scission events (open circles), or MOR (gray circles) revealed that CCSs matured more slowly when loaded with β2AR or MOR. (E) Lifetimes histograms of punctate CCSs in cells expressing β2AR before challenge (Ei), during challenge (Eii), and after washout (Eiii) of isoproterenol. Eiii insert shows increase in median lifetime of CCS lifetime on isoproteronol challenge for four cells.

($t$ = 77 s; Figure 3D) but similar to the coated bud maturation time estimated for fibroblasts under similar conditions (Taylor *et al.*, 2011). Similar to earlier data from fibroblasts, the time between CCS nucleation and the $n$th detected scission event for TfR or β2AR was roughly linear (Figure 3D). To determine whether an alternative GPCR, MOR, had a similar effect on bud maturation time, we repeated the experiment and analysis using phl-MOR and Mu2-mCherry. The MOR agonist [D-Ala$^2$, NMe-Phl$^4$, Gly-ol$^5$]-enkephalin (DAMGO) was used to trigger MOR endocytosis as described previously (Soohoo and Puthenveedu, 2013). The median time from CCS nucleation to the first detected MOR(+) scission event was ~150 s, which is approximately twice as long as the clathrin bud maturation time in cells expressing only TfR-phl.

In previous studies it was shown that the lifetime of punctate CCSs increased upon stimulation of β2AR internalization via a mechanism involving the actin cytoskeleton (Puthenveedu and von Zastrow, 2006) and receptor ubiquitination (Henry *et al.*, 2012). An analysis of overall (unclassified) spot-like CCS lifetimes revealed a similar, although moderate, increase in median spot-like CCS lifetime upon isoproterenol challenge and ligand-triggered β2AR endocytosis (Figure 3E). By inspection, the increase in median lifetime corresponded to a moderate decrease in the frequency of short-lived CCSs and consequent right shift of the lifetime distribution (compare Figure 3, Ei and Eii).

To conclude, productive CCSs in HEK293 cells, competent for β2AR internalization, comprise a markedly heterogeneous set of punctate structures and patches with a wide range of lifetimes. The great majority of productive punctate CCSs host only one scission event, but both punctate CCSs and larger patches may host multiple trains of scission events. Overall the simplest definition of a potentially productive CCS is any CCS that colocalizes with phl-β2AR after isoproterenol challenge in which the phl-β2AR is accessible to externally imposed acidification. Finally, the maturation time of productive spot-like CCSs was significantly increased by ligand-triggered β2AR or MOR internalization.

### The acute effects of ligand-triggered endocytosis on constitutive endocytosis

The dynamic relationship between constitutive clathrin-mediated endocytosis and ligand-triggered clathrin-mediated endocytosis remains only poorly characterized. It has been suggested that ~25% of CCSs preferentially internalize β2AR or TfR and ~50% internalize both β2AR and TfR (Cao *et al.*, 1998; but see von Zastrow and Kobilka, 1992) and that a specialized subset of CCSs internalize β2AR (Puthenveedu and von Zastrow, 2006). It has also been suggested that CCSs may specialize to internalize other, different types of GPCRs (Mundell *et al.*, 2006). In addition, although it is clear that β2AR clustering prolongs the lifetimes of the host coated pits (Puthenveedu and von Zastrow, 2006), it is not clear whether ligand-triggered β2AR internalization acutely affects the rate of internalization of a constitutively endocytosed receptor such as TfR. Therefore experiments were designed to explore the dynamic relationship between constitutive endocytosis of TfR and the ligand-triggered endocytosis of β2AR and to establish what proportion of TfR(+) scission events were also β2AR(+).

First, the moderately pH-sensitive red fluorescent protein mApple was inserted into the extracellular domain of β2AR to make mApp-β2AR, which, in turn, allowed simultaneous imaging of TfR-phl (to detect single constitutive endocytic events) and mApp-β2AR (to detect ligand-triggered β2AR internalization) using the pulsed pH assay. The p$K_a$ of mApple (p$K_a$ 6.5; Shaner *et al.*, 2008) is lower than that of sePhl (p$K_a$ 7.1; Sankaranarayanan and Ryan, 2000), and so a slightly more acidic wash of pH ~5.0 was used to quench both red and green fluorescence. In an example HEK293 cell bathed in buffer at pH 7.4, TfR-phl was concentrated at CCSs and otherwise distributed evenly (Figure 4Ai, green). By contrast, mApp-β2AR fluorescence was uniform, with no concentration at CCSs (Figure 4Ai, magenta). Images were acquired over a period of 400 s in conjunction with alternating pH to detect single TfR-phl(+) scission events as described. Before the addition of isoproterenol, no mApp-β2AR signal was detected at TfR-phl(+) scission events (Figure 4Bi). At $t$ = 402 s, isoproterenol was introduced into the rhythmically alternating perfusion streams to trigger mApp-β2AR endocytosis (Supplemental Figure S1 and *Materials and Methods*). After a further ~60 s, mApp-β2AR coclustered with TfR-phl at CCS, and in an example TfR-phl(+) scission event, a robust step increase in mApp-β2AR fluorescence was detected (Figure 4Bii). This could occur only if TfR-phl and mApp-β2AR pinched off in the same clathrin-coated vesicle.

To visualize the flux of β2AR through the constitutive clathrin-mediated endocytic pathway, we represented the fluorescence of bona fide TfR-phl(+) scission events as a density plot with "local time" (relative to the scission event) on the horizontal axis and "global time" (i.e., experimental time) descending on the vertical axis (Figure 4Ci) and plotted the average fluorescence of TfR-phl and mApp-β2AR before, during, and after isoproterenol challenge (Figure 4Cii). There was no detectable mApp-β2AR fluorescence at TfR (+) scission events before addition of isoproterenol, followed swiftly by a pulse of mApp-β2AR fluorescence, indicating cointernalization of β2AR with TfR into clathrin-coated vesicles (Figure 4, Ci and Cii). The fluorescence of TfR(+) scission events—which corresponds to the amount of receptor internalized by individual events—remained relatively constant for the duration of the experiment, with a moderate increase after addition of isoproterenol (Figure 4Cii, green traces). The average fluorescence of mApp-β2AR internalized per scission event rapidly decayed during exposure to isoproterenol as mApp-β2AR was depleted from the plasma membrane (Figure 4, Ci and Cii).

We established, in agreement with published results (Puthenveedu and von Zastrow, 2006), that an influx of β2AR into the clathrin-mediated endocytic machinery extended the lifetime of spot-like CCS. However, did this correspond to a general slowing of the constitutive endocytic rate? To answer this question, we measured the incidence rate of TfR-phl(+) scission events before, during, and after challenge with isoproterenol (Figure 5). In an example cluster of three cells, TfR-phl fluorescence at pH 7.4 showed a moderate decrease through the experiment, which was most likely due to bleaching (Figure 5, A and B). By contrast, mApp-β2AR fluorescence at pH 7.4 dramatically decreased with first-order kinetics upon isoproterenol addition, followed by a recovery upon washout as the mApp-β2AR was internalized and subsequently recycled (Puthenveedu and von Zastrow, 2006; Figure 5, A and C). For each cell, we defined a polygon of constant area that was contained within the footprint of the cell before, during, and after isoproterenol addition and measured the number of TfR-phl(+) scission events that occurred within the polygon over time. On addition of isoproterenol, there was a very modest, although insignificant, increase in the incidence rate of TfR-phl scission events (Figure 5D). We therefore conclude that ligand-triggered endocytosis of β2AR does not significantly change the overall incidence rate of constitutive endocytic scission events.

To conclude, mApp-β2AR internalization was detected in at least some vesicles that constitutively internalized TfR-phl, and isoproterenol-triggered mApp-β2AR endocytosis slows CCS maturation. We then sought to determine the degree of cointernalization of TfR and β2AR.

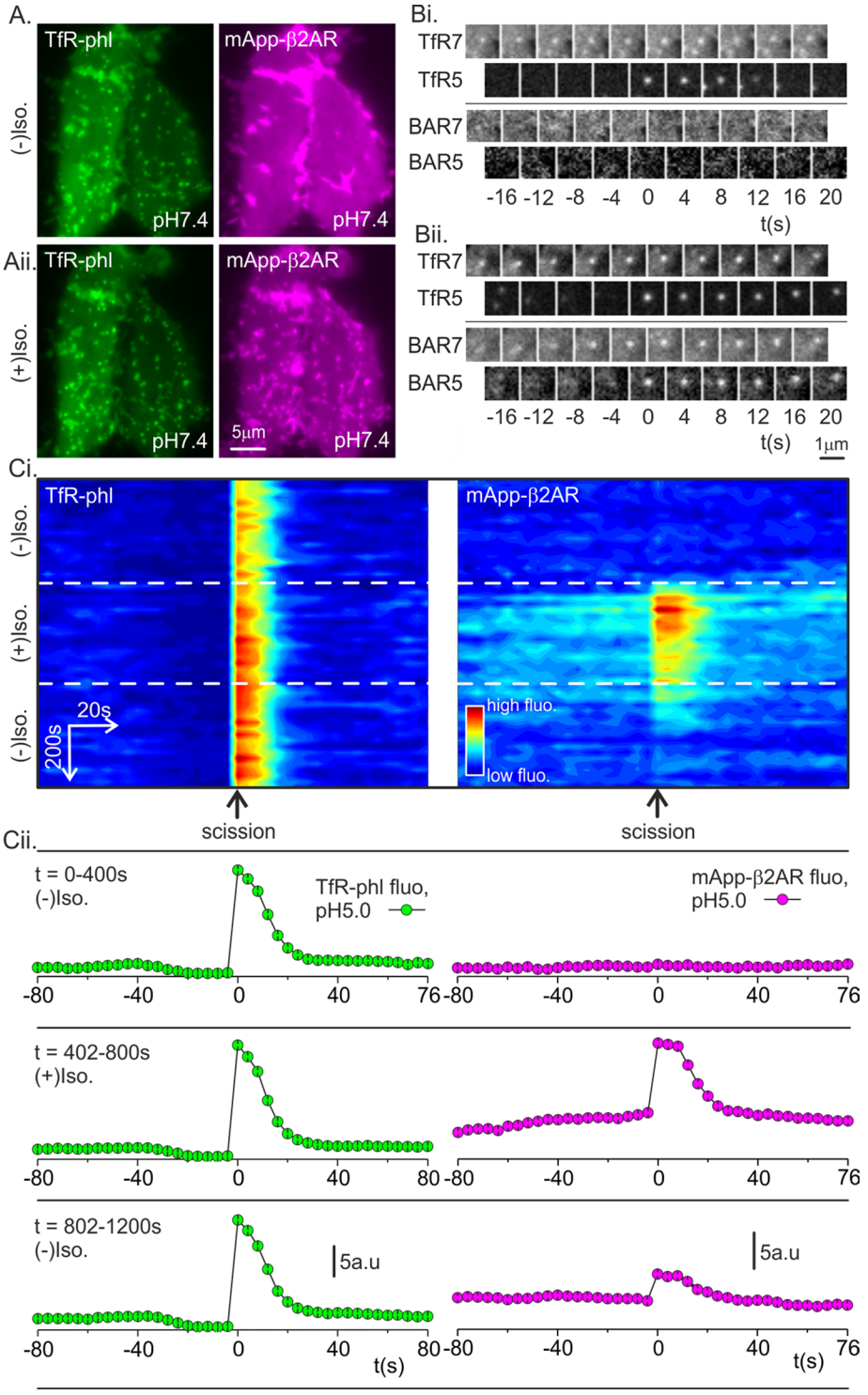


FIGURE 4: mApple-β2AR clusters and internalizes with TfR-phl. (A) Example HEK293 cell expressing TfR-phl (green, left) and mApp-β2AR (magenta, right) at pH 7.4, 50 s before isoproterenol addition (top) and 550 s after isoproterenol challenge (bottom). After isoproterenol challenge, mApp-β2AR clustered with TfR-phl at CCSs. Images are averages of 50 frames, acquired at 0.5 Hz, centered on the relative time point. (B) Example TfR-phl scission events before (Bi) and after (Bii) isoproterenol addition. After isoproterenol addition, mApp-β2AR signal coincided with TfR-phl(+) scission events, indicating that the two receptors cointernalized in the same vesicles. (Ci) Density plot of aligned fluorescence changes (horizontal axis) associated with bona fide TfR-phl(+) scission events plotted against global time (vertical axis). The flux of mApp-β2AR receptor through the constitutive CME pathway appeared as a transient pulse of fluorescence signal (right). (Cii) Quantified average fluorescence traces of TfR-phl and mApp-β2AR over the time windows indicated in Ci.

### Is there any evidence for coated-pit specialization?

In earlier work, it was shown, using immunofluorescence, that three populations of CCS exist at the plasma membrane of HEK293 cells after stimulation of β2AR internalization by isoproterenol (Cao *et al.*, 1998). Approximately ~25% of CCSs contained β2AR alone, ~50% contained both β2AR and TfR, and ~25% contained only TfR (Cao *et al.*, 1998). Here we revisited this measurement and determined the degree of coincidence of mApp-β2AR with TfR-phl in newly scissioned endocytic vesicles. To do this, we measured mApp-β2AR signal at TfR-phl(+) scission events before, during, and after isoproterenol challenge, using a quantification algorithm developed to detect very weak fluorescence changes at fluorescent puncta (see *Materials and Methods*).

We used two different approaches to estimate the proportion of TfR-phl(+)/mApp-β2AR(+) scission events. In the first method, the fluorescence of mApple-β2AR was measured at TfR-phl(+) scission events in resting cells and the fluorescence distribution used to define an upper 95% confidence limit on basal red fluorescence above which events were scored as mApp-β2AR(+) after isoproterenol challenge. For the example cell in Figure 4, 85% of TfR-phl(+) vesicles were also scored as mApp-β2AR(+) after isoproterenol challenge (see Supplemental Figure S2 for details of quantification). To verify this analysis, we manually scored TfR-phl(+) scission events for β2AR fluorescence over a window from 60 s after isoproterenol addition to the end of isoproterenol stimulation 200 s later. This analysis revealed that 89% of TfR(+) scission events were also β2AR(+) as judged by eye ($n$ = 234 events, $N$ = 3 cells).

These analysis depended on using the robust TfR-phl scission signal as a reference signal to measure constitutive scission events, and so it could not detect potential mApp-β2AR(+)/TfR-phl(–) scission events. These could correspond to scission of vesicles from "specialized" CCSs that internalized β2AR but excluded TfR. Moreover, using TfR-phl(+) scission events as a reference most likely underestimated the proportion of TfR-phl(+)/mApp-β2AR(+) scission events, as the red mApple scission signal was dimmer than the green phl signal and prone to contamination by internalized (but incompletely quenched) mApple-β2AR fluorescence. The automated scission detection algorithm was adapted to detect the very faint candidate mApp-β2AR scission events (see *Materials and Methods*). Briefly, spot fluorescence was measured

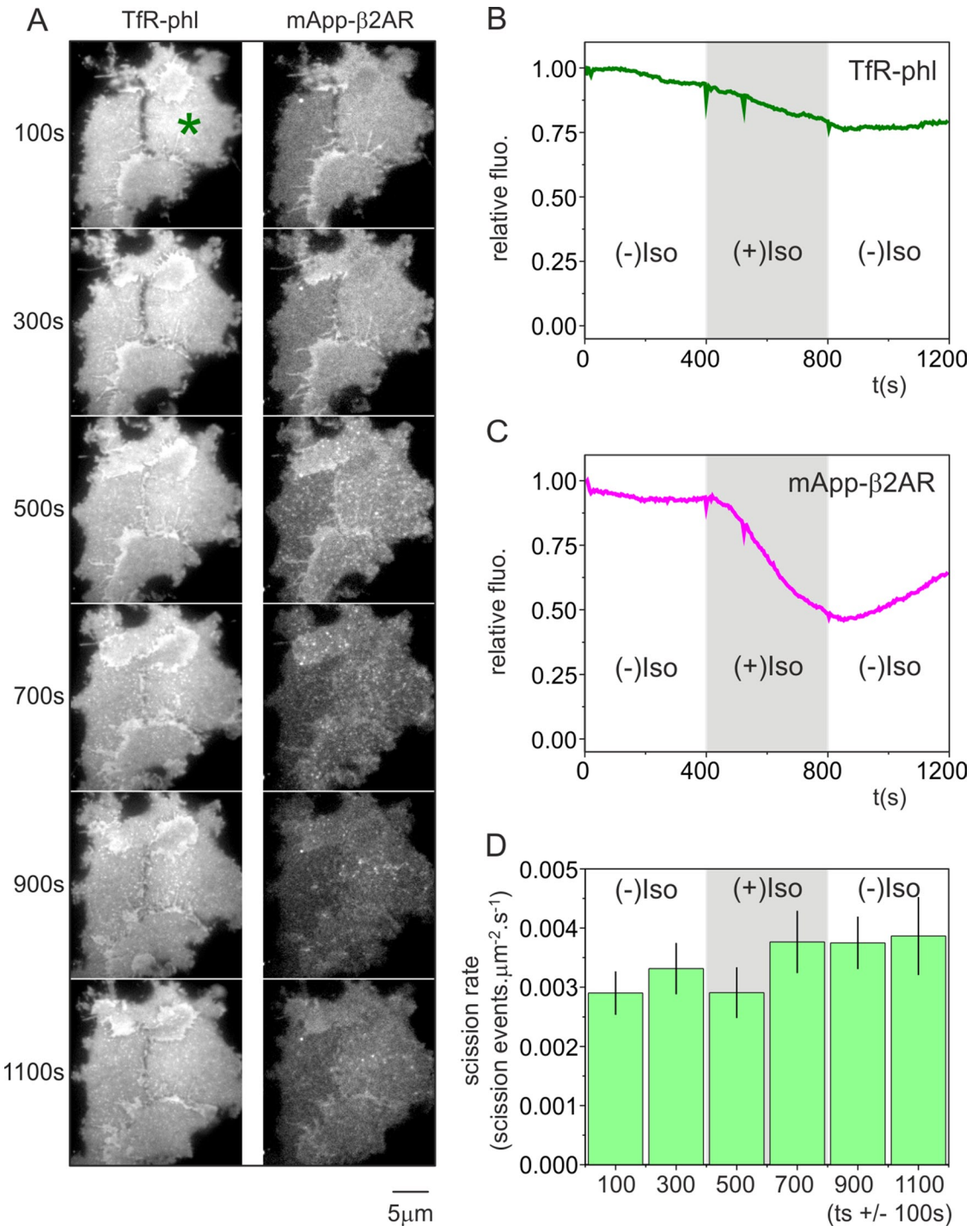


FIGURE 5: The flux of TfR-phl(+) scission events through the constitutive endocytic pathway is only mildly affected by ligand-triggered β2AR internalization. (A) A group of 3 HEK293 cells before, during, and after challenge with isoproterenol, showing surface TfR-phl fluorescence (left) and mApple-β2AR fluorescence (right) at pH 7.4. (B) Quantification of fluorescence changes in cell indicated in A by asterisk. TfR-phl fluorescence (green) showed a moderate decrease during the course of the experiment. (C) By contrast, mApple-β2AR (magenta) showed a robust decrease in fluorescence, followed by a moderate increase upon isoproterenol washout (indicated by arrow). (D) The incidence rate of TfR-phl(+) scission events, expressed as events $\mu m^{-2}$ $s^{-1}$, before, during, and after isoproterenol challenge.

using a circle-minus-annulus measurement as before, but segmented spots were excluded from the annulus measurement, giving a less noisy estimate of local background fluorescence. Candidate mApp-β2AR(+) scission events were classified as bona fide if they coincided with a cluster of mApp-β2AR at pH 7.4 and showed a stepwise fluorescence increase with S/N ≥ 10 (see *Materials and Methods*). This eliminated false-positive events, which most likely represent endocytic vesicles briefly visiting the plasma membrane. The mApp-β2AR(+) scission events identified were classified as TfR-phl(+) if there was a correlated stepwise increase in TfR-phl

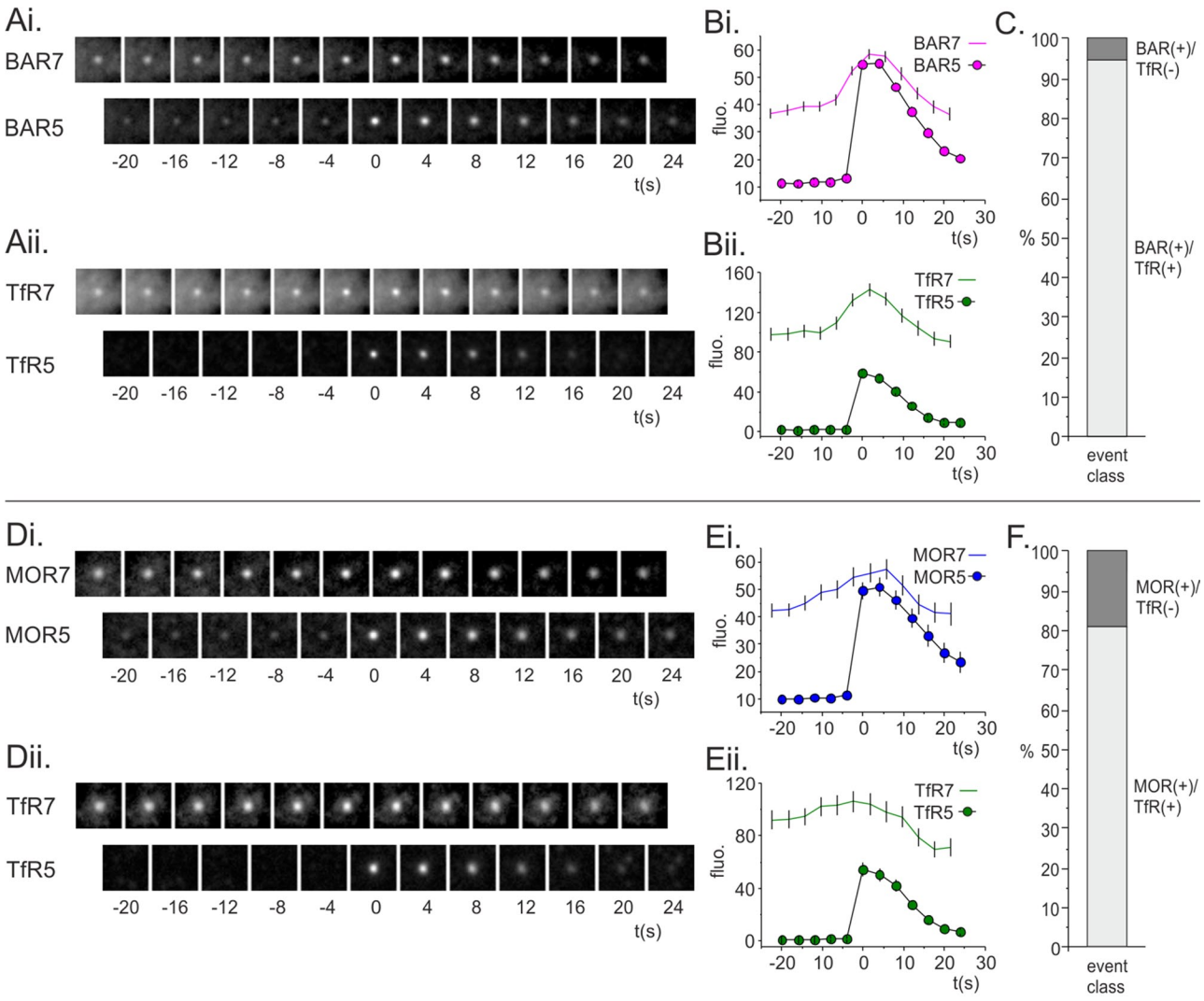


FIGURE 6: Estimating the proportion of GPCR(+)/TfR(–) scission events using either mApp-β2AR or mApp-MOR scission events as a reference. (Ai, Aii) Average time-resolved montage of mApp-β2AR(+)/TfR-phl(+) scission events. (Bi, Bii) Quantification of fluorescence at pH 5 or 7 for (Bi) mApp-BAR or (Bii) TfR-phl. (C) Ninety-five percent of mApp-β2AR(+) scission events were also TfR-phl(+). (Di, Dii) Average time-resolved montage of mAppMOR(+)/TfR-phl(+) scission events. (Ei, Eii) Quantification of fluorescence at pH 5 or 7 for (Ei) mApp-MOR or (Eii) TfR-phl. (F) Eighty-one percent of mApp-MOR(+) scission events were also TfR-phl(+).

fluorescence with S/N ≥ 5. Of the mApp-β2AR scission events identified, 95% coincided with a correlated TfR-phl(+) scission event (Figure 6, A–C). From this we conclude that, upon isoproterenol challenge, there is only one population of constitutive endocytic vesicles in HEK293 cells that internalize both mApp-β2AR and TfR-phl.

The MOR is an alternative GPCR that is believed to internalize, at least in part, from specialized CCPs, and it has been suggested that ~50% of CCPs can specialize to internalize MOR in HEK293 cells (Soohoo and Puthenveedu, 2013). To better estimate the proportion of (putative) specialized MOR(+) scission events, we made a mApp-MOR construct, coexpressed it with TfR-phl in HEK-293 cells, and performed a pulsed pH assay as for β2AR. The MOR agonist DAMGO was used to trigger MOR endocytosis as described previously (Soohoo and Puthenveedu, 2013). In general, the response of mApp-MOR to DAMGO challenge was less robust, rapid, and reproducible than the response mApp-β2AR to isoproterenol, and the imaging data were generally less satisfactory. However, on challenge with DAMGO, mApp-MOR(+) scission events were readily detected, and the proportion of mApp-MOR(+)/TfR-phl(–) scission events was estimated as for β2AR. Of the events detected (132 events, three cells), 81% were mApp-MOR(+)/TfR-phl(+), as opposed to the expected proportion of ~50% (Figure 6, D–F).

## DISCUSSION

This is, to our knowledge, the first time that ligand-triggered endocytosis has been imaged at the level of single-scission events. The parallels with a similar analysis of constitutive TfR(+) scission events in NIH3T3 fibroblasts are striking (Merrifield *et al.*, 2005; Taylor *et al.*, 2011, 2012). As for constitutive TfR endocytosis, the ligand-triggered endocytosis of β2AR proceeds via quantized scission events hosted by an apparently diverse array of clathrin spots and plaques. A simple model to explain the observed diversity of CCS dynamics is that CCSs may occur as discrete clathrin-coated buds at the

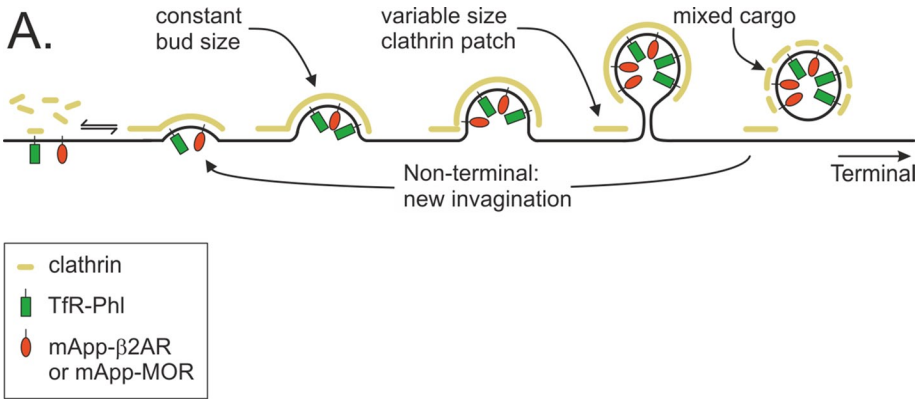


FIGURE 7: A common pathway for constitutive TfR endocytosis and ligand-triggered GPCR endocytosis. Clathrin-coated pits can internalize both TfR (green lollipops) and GPCR (β2AR or MOR; red lollipops).

plasma membrane (spot-like CCSs) or in association with a large, flat or gently curved patch of clathrin at the plasma membrane (plaque-like CCSs; Figure 7). As noted previously, the latter types of structure have been observed by electron microscopy (Heuser, 1980; Maupin and Pollard, 1983). To fully understand the CCS dynamics observed by microscopy, the dynamics of both the bud and, if present, the associated clathrin patch must be considered. If the patch of clathrin at the membrane is absent, the coated bud will disappear once scission occurs in a terminal event (Figure 7). If a small patch of clathrin is left after scission, a nonterminal event will occur if a fresh bud regrows at the same site (Figure 7). If the associated patch is sufficiently large and perhaps stabilized by adhesion (Batchelder and Yarar, 2010), it might sufficiently bright to obscure the loss of clathrin coat during budding events at or close to its edges, which would thus evade detection by conventional fluorescence microscopy, and it would appear as a plaque (Figure 7). Therefore CCSs are superficially heterogeneous even though they represent a common pathway of receptor internalization.

Similar to an earlier study (Puthenveedu and von Zastrow, 2006), it was found that ligand-triggered β2AR internalization moderately extends the lifetime of spot-like CCS by ~53%. Here a prolongation of spot-like CCS lifetime was found using two different analyses: first, by tracking all spot-like CCSs before, during, and after ligand-triggered β2AR endocytosis in the same set of cells, and second, by comparing the time between spot-like CCS nucleation and the first detected scission event for β2AR(+), MOR(+), or TfR(+) scission events in different sets of cells. It has been proposed that the prolongation of spot-like CCS lifetime by β2AR loading may be of functional significance, perhaps reflecting the dynamics of a specialized subset of CCSs (Puthenveedu and von Zastrow, 2006; Henry *et al.*, 2012). Here, by simultaneously detecting the presence of TfR and β2AR in newly scissioned vesicles, it was shown that β2AR does increase the lifetime of CCSs but that TfR and β2AR internalize in the same vesicles budding from CCSs. Moreover, despite the change in bud maturation time, the incidence rate of scission events remained remarkably constant before, during, and after ligand-triggered β2AR endocytosis. One possible explanation for the steady flux is that the number of CCSs increases in response to ligand-triggered endocytosis and so compensates for increased bud maturation time. Indeed, in an example cell expressing Mu2-mCherry and phl-MOR, the number of detected CCSs significantly increased after DAMGO stimulation (Supplemental Figure S3). Therefore the increase in CCS maturation time may be offset by simply nucleating more CCSs. It was also found that the amount of TfR-phl internalized by scission events changed little—and if anything slightly increased—when mApp-β2AR was driven through the clathrin-mediated endocytic pathway, suggesting that although the two receptors internalized in the same vesicles, they did not compete with one another.

When the coincidence of Tfr-phl and mApp-MOR at endocytic events was analyzed, it was found that ~19% of scission events were mApp-MOR(+)/TfR-phl(–), which was a substantially lower proportion than the expected ~50% (Soohoo and Puthenveedu, 2013). These results therefore favor a model in which activated β2-AR and MOR hitchhike into the cell via constitutively internalizing clathrin-coated pits but can nonetheless modify the maturation times of the host CCSs (Figure 7). It remains possible that the ~19% of scission events that apparently internalized MOR but not TfR represent specialized CCSs. However, as noted, detection limits and the possibility of false-positive TfR-phl(–)/mApp-MOR(+) must be kept in mind when considering this possibility. In the future, a similar experimental strategy may be used to determine whether other types of receptor enter the cell via the same or specialized CCSs.

## MATERIALS AND METHODS

### TIRFM and perfusion system

The dual-color TIRFM microscope has been described previously (Taylor *et al.*, 2011). The four- channel perfusion system was based on a previously published design (Taylor *et al.*, 2011) with the addition of three-way miniature valves to control addition/washout of drugs (part LFRX0500050B; Lee Company, Westbrook, CT). All control and switching electronics were designed and built in-house.

### Pulsed pH assay

The pulsed pH assay was described previously (Merrifield *et al.*, 2005) and in more detail here in Supplemental Figure S1. Briefly, the perfused buffer was switched between pH 7.4 (HBS: 135 mM NaCl, 5 mM KCl, 1.8 mM $CaCl_2$, 0.4 mM $MgCl_2$, 1 mM D(+)-glucose, 25 mM 4-(2-hydroxyethyl)-1-piperazineethanesulfonic acid, 2% fetal calf serum [FCS]) and pH 5.0 (MBS: 135 mM NaCl, 5 mM KCl, 1.8 mM $CaCl_2$, 0.4 mM $MgCl_2$, 1 mM D(+)-glucose, 25 mM 2-(*N*-morpholino)ethanesulfonic acid, 2% FCS). To trigger β2AR internalization, 20 mM isoproterenol was added to both HBS and MBS streams. All chemicals were bought from Sigma-Aldrich (St. Louis, MO).

### Cell culture and transfection

HEK293 cells were grown DMEM (Life Technologies SAS, St. Aubin, France) supplemented with 10% fetal bovine serum in 10% $CO_2$ and at 37°C. Adherent HEK293 cells, growing in six-well plates, were transfected with the relevant plasmid(s) using Lipofectamine 2000 at 24–48 h before imaging experiments and as per manufacturer's instruction (Invitrogen, Carlsbad, CA). Cells were replated onto clean coverslips ~4 h after transfection and allowed to adhere overnight ready for imaging the following morning.

### Glass cleaning

Coverslips were cleaned as described previously (Merrifield *et al.*, 2005; Taylor *et al.*, 2011). Briefly, coverslips were washed thrice in wash solution (0.01% DECON 90 [Decon Laboratories, Hove, United

Kingdom]) and 100 mM KOH, thoroughly rinsed in double-distilled $H_2O$, washed once in 100% EtOH, and washed once in acetone before air drying in a sterile hood. All chemicals were supplied by Sigma-Aldrich unless otherwise stated.

### Plasmid design and construction

The design of TfR-phl has been described previously (Merrifield *et al.*, 2005). The yellow fluorescent protein (YFP) of YFP-β2AR (Dorsch *et al.*, 2009) was replaced with super-ecliptic pHluorin using the *Bam*HI and *Xba*I restriction sites (super-ecliptic pHluorin was amplified with the primers AAAAAGGATCCATGAAGACGATCATCGCCCTGAGCTACATCTTCTGCCTGGTATTCGCCAGTAAAGGAGAAGAACTTTTCACTGGAGTTGTCCC [also encoding a hemagglutinin signal sequence; Guan *et al.*, 1992] and AAAAATCTAGATTTGTATAGTTCATCCATGCC). Phluorin was replaced with mApple to make mApple-β2AR using two sequential PCR reactions to reengineer the human growth hormone signal sequence into the N-terminus of mApple. To generate mApple-MOR, the entire open reading frame (ORF) of human MOR was synthesized (Eurofins MWG, Ebersberg, Germany) with appropriate 5′ and 3′ restriction sites and used to replace the β2AR ORF in phl-β2AR and mApp-β2AR. The Mu2 construct was described previously (Taylor *et al.*, 2011). Briefly, mCherry was inserted within the rat Mu2 ORF at residue 236 using the *Bgl*II and *Nde*I sites (plasmid 27672; Addgene, Cambridge, MA).

### Image analysis

All image analysis was performed in Matlab (MathWorks, Cambridge, United Kingdom) using custom-written software as described previously (Taylor *et al.*, 2011), with the following modifications. Scripts were written in Matlab to segment spots using the wavelet-based multiscale products as described previously (Olivo-Marin, 2002). The coordinates of spots were extracted in Matlab and track histories generated using a Matlab version of the IDL nearest-neighbor algorithm (www.physics.emory.edu/~weeks/idl/). To detect the very faint mApp-β2AR (+) scission events, the fluorescence of candidate spots was quantified using a circle-minus-annulus measurement in which segmented spots were excluded from the annulus. This eliminated a major source of noise in the fluorescence measurement and allowed a more accurate estimate of fluorescence.

## ACKNOWLEDGMENTS

We acknowledge funding from Medical Research Council (MRC, London, UK) grant MC_U105178789 and Fondation pour la Recherche Medicale (FRM, Paris, France) grant AJE201108.

## REFERENCES

Batchelder EM, Yarar D (2010). Differential requirements for clathrin-dependent endocytosis at sites of cell-substrate adhesion. Mol Biol Cell 21, 3070–3079.

Burd C, Cullen PJ (2014). Retromer: a master conductor of endosome sorting. Cold Spring Harb Perspect Biol 6, a016774.

Cao TT, Mays RW, von Zastrow M (1998). Regulated endocytosis of G-protein-coupled receptors by a biochemically and functionally distinct subpopulation of clathrin-coated pits. J Biol Chem 273, 24592–24602.

Dorsch S, Klotz KN, Engelhardt S, Lohse MJ, Bunemann M (2009). Analysis of receptor oligomerization by FRAP microscopy. Nat Methods 6, 225–230.

Ehrlich M, Boll W, Van Oijen A, Hariharan R, Chandran K, Nibert ML, Kirchhausen T (2004). Endocytosis by random initiation and stabilization of clathrin-coated pits. Cell 118, 591–605.

Guan XM, Kobilka TS, Kobilka BK (1992). Enhancement of membrane insertion and function in a type IIIb membrane protein following introduction of a cleavable signal peptide. J Biol Chem 267, 21995–21998.

Henry AG, Hislop JN, Grove J, Thorn K, Marsh M, von Zastrow M (2012). Regulation of endocytic clathrin dynamics by cargo ubiquitination. Dev Cell 23, 519–532.

Heuser J (1980). Three-dimensional visualization of coated vesicle formation in fibroblasts. J Cell Biol 84, 560–583.

Keyel PA, Mishra SK, Roth R, Heuser JE, Watkins SC, Traub LM (2006). A single common portal for clathrin-mediated endocytosis of distinct cargo governed by cargo-selective adaptors. Mol Biol Cell 17, 4300–4317.

Loerke D, Mettlen M, Yarar D, Jaqaman K, Jaqaman H, Danuser G, Schmid SL (2009). Cargo and dynamin regulate clathrin-coated pit maturation. PLoS Biol 7, e57.

Maupin P, Pollard TD (1983). Improved preservation and staining of HeLa cell actin filaments, clathrin-coated membranes, and other cytoplasmic structures by tannic acid-glutaraldehyde-saponin fixation. J Cell Biol 96, 51–62.

Merrifield CJ, Feldman ME, Wan L, Almers W (2002). Imaging actin and dynamin recruitment during invagination of single clathrin-coated pits. Nat Cell Biol 4, 691–698.

Merrifield CJ, Perrais D, Zenisek D (2005). Coupling between clathrin-coated-pit invagination, cortactin recruitment, and membrane scission observed in live cells. Cell 121, 593–606.

Miesenbock G, De Angelis DA, Rothman JE (1998). Visualizing secretion and synaptic transmission with pH-sensitive green fluorescent proteins. Nature 394, 192–195.

Mooren OL, Galletta BJ, Cooper JA (2012). Roles for actin assembly in endocytosis. Annu Rev Biochem 81, 661–686.

Mundell SJ, Luo J, Benovic JL, Conley PB, Poole AW (2006). Distinct clathrin-coated pits sort different G protein-coupled receptor cargo. Traffic 7, 1420–1431.

Olivo-Marin JC (2002). Extraction of spots in biological images using multiscale products. Pattern Recognition 35, 1989–1996.

Puthenveedu MA, Lauffer B, Temkin P, Vistein R, Carlton P, Thorn K, Taunton J, Weiner OD, Parton RG, von Zastrow M (2010). Sequence-dependent sorting of recycling proteins by actin-stabilized endosomal microdomains. Cell 143, 761–773.

Puthenveedu MA, von Zastrow M (2006). Cargo regulates clathrin-coated pit dynamics. Cell 127, 113–124.

Rappoport JZ (2008). Focusing on clathrin-mediated endocytosis. Biochem J 412, 415–423.

Saffarian S, Cocucci E, Kirchhausen T (2009). Distinct dynamics of endocytic clathrin-coated pits and coated plaques. PLoS Biol 7, e1000191.

Sankaranarayanan S, Ryan TA (2000). Real-time measurements of vesicle-SNARE recycling in synapses of the central nervous system. Nat Cell Biol 2, 197–204.

Shaner NC, Lin MZ, McKeown MR, Steinbach PA, Hazelwood KL, Davidson MW, Tsien RY (2008). Improving the photostability of bright monomeric orange and red fluorescent proteins. Nat Methods 5, 545–551.

Soohoo AL, Puthenveedu MA (2013). Divergent modes for cargo-mediated control of clathrin-coated pit dynamics. Mol Biol Cell 24, 1725–1734, S1721–1712.

Staehelin M, Simons P (1982). Rapid and reversible disappearance of beta-adrenergic cell surface receptors. EMBO J 1, 187–190.

Taylor MJ, Lampe M, Merrifield CJ (2012). A feedback loop between dynamin and actin recruitment during clathrin-mediated endocytosis. PLoS Biol 10, e1001302.

Taylor MJ, Perrais D, Merrifield CJ (2011). A high precision survey of the molecular dynamics of mammalian clathrin-mediated endocytosis. PLoS Biol 9, e1000604.

Tosoni D, Puri C, Confalonieri S, Salcini AE, De Camilli P, Tacchetti C, Di Fiore PP (2005). TTP specifically regulates the internalization of the transferrin receptor. Cell 123, 875–888.

von Zastrow M, Kobilka BK (1992). Ligand-regulated internalization and recycling of human beta 2-adrenergic receptors between the plasma membrane and endosomes containing transferrin receptors. J Biol Chem 267, 3530–3538.